

RESEARCH ARTICLE

Design of a Low Voltage and High Power Traveling Wave Tube Based on a Sheet-Beam Rectangular Ring-Bar Slow-Wave Structure

G. PATERNA¹, G. LIPARI¹, E. TRAINA¹, G. COMPARATO, A. MURATORE¹,
P. LIVRERI¹, (Senior Member, IEEE), S. STIVALA¹, AND A. BUSACCA¹

Department of Engineering, University of Palermo, 90128 Palermo, Italy

Corresponding authors: A. Busacca (alessandro.busacca@unipa.it) and S. Stivala (salvatore.stivala@unipa.it)

ABSTRACT In this article, a sheet-beam type ring bar slow wave structure (RBSWS) capable of working at very low-voltage value is proposed. The structure is designed to work over the frequency range from 14 to 18 GHz with a cathodic voltage of 2.050 kV and a current of 100 mA. Simulation results for two 50-period sections, carried out by CST Studio Suite 2023, show a saturated output power of 30 W, a maximum gain of 0.795 dB/mm, and a radio frequency (RF) electronic efficiency higher than 15 %. The proposed structure is ideal for aerospace applications that usually require compact size, low weight and power consumption, while maintaining very high output power levels. Furthermore, this device is relatively easy to manufacture, making it a more accessible option than other structures that require complex and expensive manufacturing processes. Finally, the mechanical and thermal dissipation problems are kept under control thanks to the large surface contact between the slow wave structure and the dielectric rod realized in Boron Nitride.

INDEX TERMS High power amplifiers, traveling wave tubes, sheet-beam, low operating voltage, ring bar.

I. INTRODUCTION

Vacuum tubes are a particular class of amplifiers, using an electron beam to amplify or generate signals with an operating frequency up to 300 GHz. Among the different types of vacuum tubes, the most relevant are Klystrons, Traveling Wave Tubes (TWTs), and cross-field devices, each one of them possessing a specific structure and a different working principle [1], [2], [3], [4], [5], [6], [7], [8], [9], [10], [11], [12], [13]. In particular, TWTs are a class of linear vacuum tubes in which an electron beam travels inside or in the proximity of a periodic structure. The latter reduces the phase velocity of the electromagnetic wave generated by the RF signal, allowing to achieve the synchronism condition between the wave and the electron

beam. When such a synchronism condition is achieved, the energy transfer from the electron beam is used to amplify the RF signal. With regard to the interaction structure geometry, TWTs usually employ a circular section and, hence, circular beams are required in order to obtain the best interaction [1]. Nevertheless, the use of a rectangular beam has several advantages. If compared to a conventional circular beam, a sheet-beam usually allows to achieve a stronger interaction impedance, as well as higher gain, output power and electronic efficiency for the same voltage and current, thus reducing the overall power consumption of the device [3]. Moreover, it is possible to increase the current and, at the same time, to maintain stable the beam density, simply by increasing the beam cross-section area [4]. Finally, these devices are more compact and lighter when compared to conventional TWTs [5]. All these characteristics are fundamental for aerospace applications, in which one

The associate editor coordinating the review of this manuscript and approving it for publication was Vittorio Camarchia¹.

of the main goals is to minimize both power consumption and weight. In the last years, several configurations of sheet-beam TWTs have been proposed [6], [7], [8], [9], [10], [11], [12], [13]. Some of them are able to operate with a very low voltage, such as the one proposed by Wen et al. [10]: a concentric arc meander line capable of operating with a voltage of 720 V. A similar configuration, able to work with a voltage of 791 V, has been proposed by Wang et al. [11]. All these configurations are compact, lightweight and efficient, and represent valid alternatives to classical TWTs or solid-state devices. However, the manufacturing aspect is undoubtedly a limiting factor, since, these configurations can only be realized by means of micro-fabrication techniques. In fact, the mentioned structures work at relatively high frequencies and, for this reason, they have particularly small dimensions, very difficult to be realized with conventional techniques (such as electrical discharge machining, EDM).

Moreover, the gain per unit length of these structures is relatively low and most of them are subject to mechanical stability and thermal dissipation problems. In a previous work, we proposed a Planar Helix with Straight-Edge Connection (PH-SEC) capable of reaching an output power of 5.5 W at 20 GHz with a working voltage of 1.7 kV [14]. Despite the simple geometry for the proposed PH-SEC, it is still of difficult realization and presents some mechanical and thermal limitations [15]. The ring bar structure is a modification of the classic contra-wound bifilar helix [19] and usually has a larger diameter for the same working frequency, thus allowing for an easier fabrication process. Furthermore, this slow-wave structure exhibits a higher interaction impedance for the fundamental forward wave than for the backward one. Thanks to these properties, if compared to helix SWS, the ring bar structure is able to provide higher levels of output power over a narrower bandwidth, that can anyway reach values of several GHz [16]. In this work, we propose a rectangular ring bar (RRB) SWS [17], [18], [19] which combines the advantages of a simple manufacturing process and a high gain.

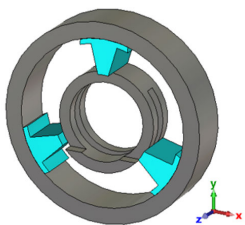


FIGURE 1. CST schematic view of the fundamental cell of the RBSWS.

The RRB was proposed for the first time by C. Chua et al. [17], who demonstrated its multiple advantages if compared to similar planar structures, including the aforementioned PH-SEC. Moreover, the results reported in [17] allow to make a qualitative assessment for similar structures, even operating in a different frequency range.

Nevertheless, it is difficult to extrapolate from [17] both the dimensions and the performance of a structure with a very different aspect ratio and operating at a different voltage, such as the one proposed in this paper. Other examples of rectangular ring bar have been also investigated [18], [19], [20]. Table 1 shows a comparison between the RRB presented in this work and the most significant structures already reported in the literature, in the field of RRBs and low voltage SWSs. In our work, we have designed and simulated a RRBSWS able to operate with a cathodic voltage of 2 kV over a frequency range spanning from 14 GHz to 18 GHz. This structure represents a more viable option, in terms of implementation, than other SWS since it can be easily fabricated by EDM techniques. Moreover, the use of a large dielectric rod allows to avoid mechanical and thermal problems, thus allowing high RF power operation. As evident from Table 1, our structure is aimed at minimizing power consumption (since it requires a very low operating voltage) and shows a very compact size and the highest gain per unit length if compared to the other entries, without considering our previous work [14] in which, however, the output power is significantly lower (5.5 W vs. 30 W). This article is organized as follows. In section II, the design criteria of RRBSWS are proposed. In section III, the dispersion diagram, interaction impedance and the Brillouin diagram for both a circular and a rectangular ring bar are shown and compared. Moreover, in this section, the transmission characteristics of a 50-period structure are evaluated for the RRBSWS. In this case, a simple coupler geometry is considered. Finally, in section IV the results of the beam-wave interaction for the proposed structure are discussed.

II. PROPOSED STRUCTURE

In Fig. 2, the schematic view of our modified SWS is shown.

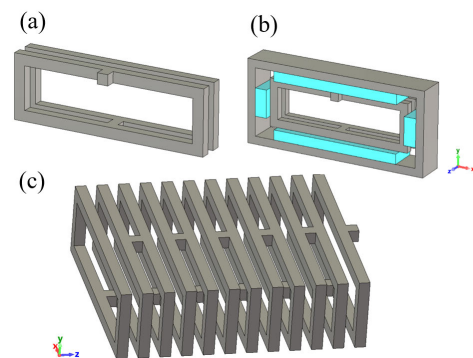


FIGURE 2. (a) CST schematic view of the periodic structure of the fundamental cell. (b) Fundamental cell with dielectric and external housing. (c) Six cells SWS.

The project requirements are listed in Table 2. As for the design criteria, we considered to find the pitch and the perimeter of the structure by considering to approximate the RRBSWS to a helix and to use these values for a preliminary dimensioning.

TABLE 1. Comparison between low voltage SWS and RRB.

Type of SWS [Ref.]	Frequency range	V_k	Current	P_{out}	Electronic efficiency	Gain p.u. lenght	Width x Height	Axial length
Units	(GHz)	(kV)	(A)	(W)	(%)	(dB/mm)	(mm ²)	(mm)
meander line [10]	24-42	0.72	0.2	40	30.6	-	-	-
meander line [11]	20-45	0.79	0.3	60	25.9	-	-	-
PH-SEC [14]	20	1.7	0.015	5.5	21	1.2	4.39 x 0.420	29
RRB [17]	80-110	-	-	-	-	-	-	-
RRB [18]	90-98	19.7	0.02	28.6	15.7	0.73	1.27 x 2.54	33
RRB [19]	27-37	25.1	0.2	581	11.57	0.366	2.12 x 1.18	111
RRB [20]	28.5-35.5	15.7	0.23	695	19.26	0.623	1.29 x 0.74	70
RRB [This works]	14-18	2	0.1	30	15	0.795	2.2 x 0.8	40

TABLE 2. Project requirement of the proposed structure.

f = 14-18 GHz	$V_c = 2-3$ kV	Gain = 30 dB	$\eta \geq 10$ %	$L \leq 5$ cm
---------------	----------------	--------------	------------------	---------------

Referring to Table 2. V_c is the accelerating cathodic voltage, η is the electronic efficiency and L is the length of the structure. Such as for the classical helix, the operational frequency depends on the phase velocity of the structure, which in turns depends mostly on its periodicity. For the initial design, we considered the circular helix equations. The main condition for obtaining amplification is the achievement of synchronism, which means that the velocity of the electrons in the beam must be almost equal to the phase velocity of the RF signal, as reported in equation (1).

$$v_p \approx v_0 \tag{1}$$

where v_p is the phase velocity of the signal in the slow wave structure, while v_0 is the velocity of the electrons. Starting from the cathodic voltage requirements, we can obtain an approximate value of the electron velocity. In fact, this value can be found by the energy conservation equation (2).

$$\frac{1}{2}mv_0^2 = eV_c \tag{2}$$

where m and e are the mass and the charge of the electron, respectively. The value of electron velocity and, consequentially, the phase velocity at the synchronism condition has been found to be 0.088 c (being c the speed of light in vacuum). Theoretically, the best degree of interaction is reached for the frequency corresponding to a normalized phase constant of 0.5 in the Brillouin diagram. This condition can be mathematically expressed by the equation (3).

$$\frac{\omega L}{v_0 \pi} = 0.5 \tag{3}$$

where $\omega = 2\pi f$, being f the working frequency, and L is the periodicity of the structure. Using equation (3) we found L to be equal to 0.4 mm at the center frequency f = 16 GHz. The next important parameter to be found is the perimeter of the slow wave structure. For a classical helix,

this can be derived as a function of the pitch angle Ψ , as in equation (4).

$$\tan(\Psi) = \frac{L}{2\pi a} \tag{4}$$

in which $2\pi a$ is the perimeter of the helix. For our approximation, we have considered the perimeter of the proposed structure equal to that of the helix. This value has been calculated to be equal to 4.5 mm. Starting from these values the SWS has been designed. Considering the power levels at which the structure should work and the dimensions of the structure itself, it is necessary to use materials with a high melting point, such as molybdenum or tungsten. Instead, the outer shell can be realized in copper. In our simulations, the outer waveguide is made of copper (electrical conductivity $\sigma = 58 \cdot 10^6$ S/m, melting point T = 1085 °C), while the material chosen for the SWS and the couplers is molybdenum ($\sigma = 18.7 \cdot 10^6$ S/m, melting point T = 2623 °C). The dielectric employed for the support rods is boron nitride (BN), which has a dielectric constant of 4.6 at a frequency of 8.8 GHz, with a thermal conductivity of 20-27 W/m K. The large contact surface between the slow wave structure and the dielectric rods guarantees a high mechanical stability and thermal dissipation [21]. In order to meet the project requirements, a sweep of simulations has been performed aimed at optimizing both the periodicity and the perimeter of the structure, as well as the dielectric rod dimensions. Despite the initial approximation, the final values do not differ much from the starting ones. In Fig. 3 the structure of the fundamental cell with its dimensions is shown.

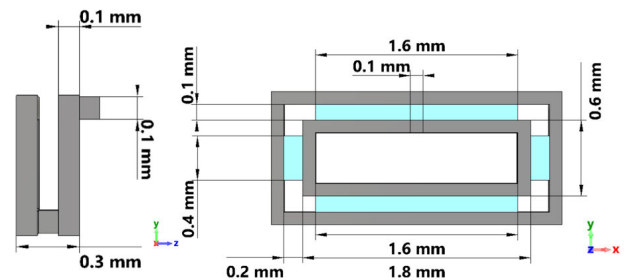


FIGURE 3. Lateral and frontal views of the fundamental cell of the RRBSWS with its dimensions.

III. COLD-TEST PARAMETERS RESULTS

The proposed structure has been compared to a circular section ring-bar. Its dimensions have been defined with the same criteria used for its planar counterpart. The interaction impedance, Brillouin diagram and dispersion characteristics for both the (circular) RBSWS and the RRBSWS are shown in figures 4, 5 and 6, respectively.

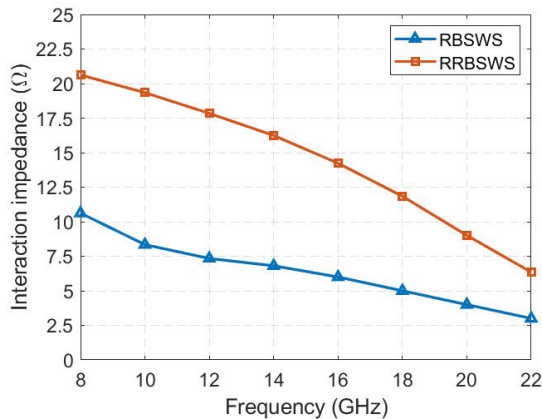


FIGURE 4. Interaction impedance of the circular RBSWS (blue triangles) and RRBSWS (orange squares).

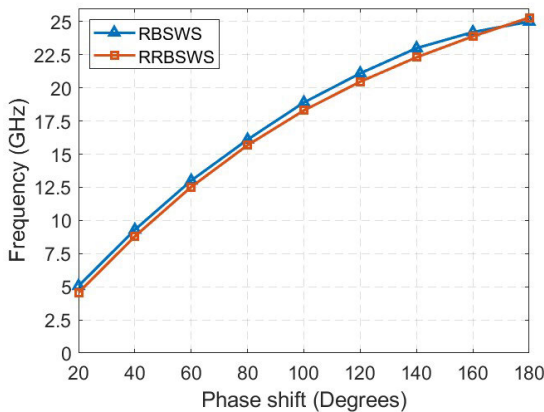


FIGURE 5. Brillouin diagram of the circular RBSWS (blue) and rectangular RRBSWS (orange).

As depicted in Fig. 4, in the frequency range of interest, the RRBSWS shows a higher interaction impedance (evaluated as the average across the cross section of the SWS). In fact, in the 14 - 18 GHz range, the value shown by the RRBSWS varies from 15 to 11 Ω , while for the counterpart it varies from 6 to 3 Ω . The Brillouin diagram (Fig. 5) shows the capability of both structures to work at the desired frequency range. In particular, the best degree of interaction for the rectangular one should be obtained for 17 GHz. In addition, the phase velocity (Fig. 6) is flatter for the RRBSWS allowing for a more stable interaction along a wider range of frequencies. The lower degree of dispersion and the overall higher interaction impedance should allow for a stronger coupling between the beam

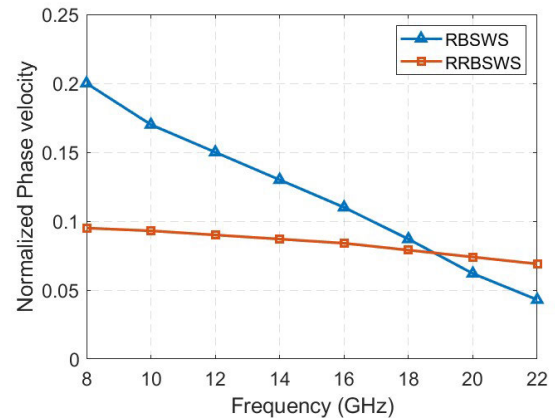


FIGURE 6. Dispersion characteristics of the circular RBSWS (blue) and RRBSWS (orange).

and the RF signal and, hence, the output signal can reach higher power levels. Having established the advantages of the RRBSWS over the RBSWS, we have studied the transmission characteristics of a structure composed of 50 fundamental cells with two electrical ports realized by two simple rectangular couplers. The whole structure is surrounded by a rectangular guide, used as an external housing, as shown in Fig. 7.

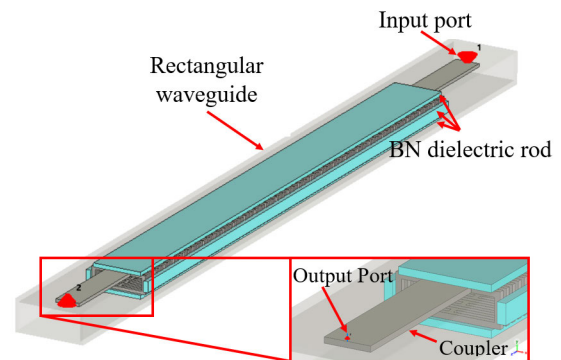


FIGURE 7. 50 periods slow wave structure with detail of couplers.

The S-parameter analysis has been performed using discrete ports and taking in account the RF losses of all the materials. Both their characteristic impedance (70 Ω) and the dimensions of the couplers ($0.8 \times 3 \times 0.1$ mm) have been chosen for matching purposes, i.e. to reduce the reflection coefficient at the input port and maximize the transmission to the output port. The final results of this process are shown in Fig. 8. The optimization process has allowed to obtain a S_{11} parameter smaller than -10 dB and a S_{21} parameter higher than -1 dB in the frequency range of interest.

IV. HOT-TEST PARAMETERS RESULTS

In order to simulate the proposed RRBSWS in terms of hot-test parameters, we employed a structure composed by two

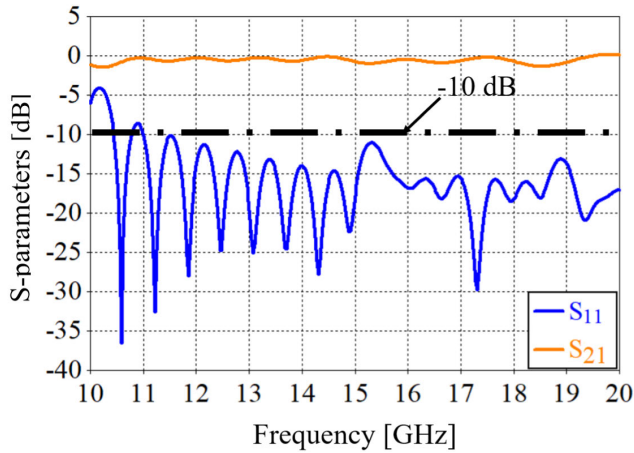


FIGURE 8. S-parameters of the 50 period structure.

sections of 50 periods each, as shown in Fig. 9. The RF signal is applied to the input port of the first section and is extracted from the output port of the second one, while the output port of the first section and the input port of the second one are terminated using two matched loads (modeled as “discrete ports” with an impedance of 70 Ω), thus providing an idealized version of a sever. For these simulations, the cathode is a parallelepiped with a thickness of 0.5 mm and an emitting surface of 1.3 × 0.225 mm². In this condition, the filling factor of the beam inside the slow wave structure is equal to 45% and with a beam current density of 34.18 A/cm². The cathodic accelerating voltage and current are equal to 2.050 V and 0.1 A respectively. The theoretical minimum value of the focusing magnetic field (i.e., the Brillouin magnetic field, B_{Bri}) for a sheet electron beam can be expressed by means of equation (5) [22].

$$B_{Bri} = \sqrt{\frac{\sqrt{2}I_0}{wt\gamma\epsilon\eta^{3/2}V_0^{1/2}}} \tag{5}$$

where ϵ is the vacuum permittivity, w and t are the width and thickness of the beam, respectively, γ is the relativistic factor, and η is the charge-to-mass ratio. By substituting all the parameters in equation (5), the minimum value of the focusing magnetic field results to be equal to 0.0156 T. Anyway this is solely a theoretical minimum value, which requires to be optimized. In fact, our simulations proved that if we use this value, the electron beam is not correctly focused and hits the SWS, thus preventing the proper functioning of the TWT. For this reason, we have gradually increased the magnetic field and the optimum results were obtained for a uniform focusing magnetic field of 0.45 T along the entire structure. With this value, the electron beam transmission coefficient at the end of the second section is equal to 100%.

The overall length of the proposed structure, taking into account both the input and output couplers, is 4.52 cm.

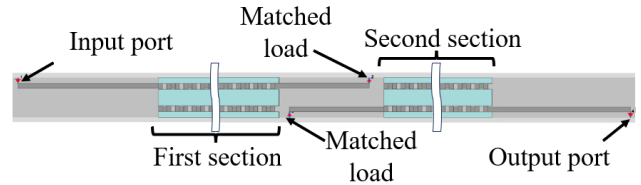


FIGURE 9. CST schematic view of the proposed structure.

In Table 3 the main electrical and geometrical parameters of the double section RRB are listed.

TABLE 3. Electrical and geometrical parameters of the two sections RRB.

Cathodic voltage	2.050 kV
Beam current	0.1 A
Beam cross section	1.3 × 0.225 mm ²
Beam current density	34.18 A/cm ²
Filling factor	0.45
Input power	0.020 W
Magnetic field	0.45 T
Number of fundamental cells	100
Overall length	4.5 cm

For this structure, in the case of an input signal with a power of 20 mW and a frequency of 17 GHz, an output signal with a power of 30 W with a transient time of 5 ns was obtained. As shown in Fig. 10, there is no disturbance on the output signal when the steady state condition is reached.

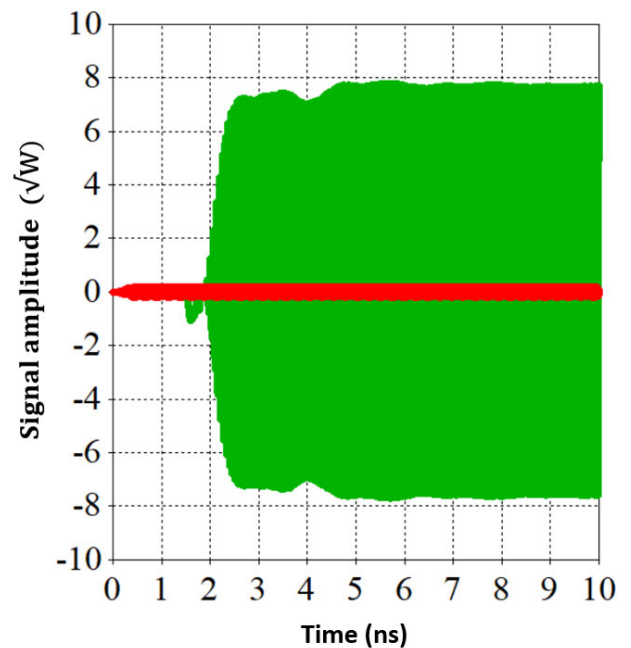


FIGURE 10. Input (red) and output signal (green) from the RRBSWS at 17 GHz.

The spectrum of both the input and output signal have been obtained by means of Fast Fourier Transform (FFT) and are shown in Fig. 11. It can be noticed that it is very

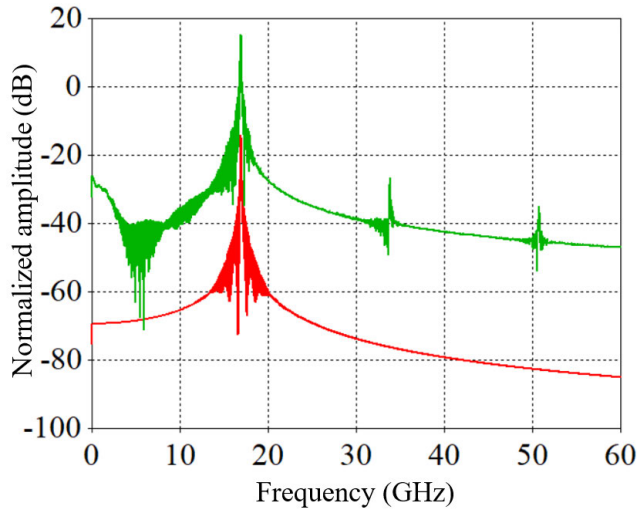


FIGURE 11. FFT of the input (red) and output (green) signals in the proposed RRBSWS.

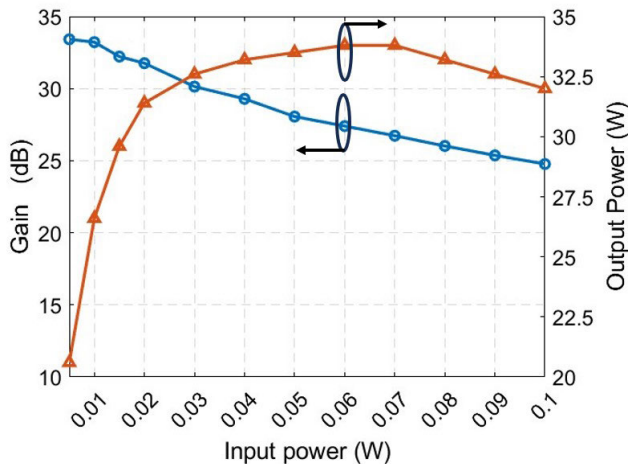


FIGURE 12. Gain (blue) and Output Power (orange) Vs input power.

clear and the higher order harmonics have an amplitude smaller than 30 dB if compared to the fundamental one. In such conditions, oscillations and instability should be highly suppressed, guaranteeing for the stability of the TWT.

In Fig. 12 gain and output power at the varying of the input power, for a fixed frequency of 17 GHz, are reported. Fig. 13, instead, shows gain and output power of the RRBSWS as a function of the frequency, under the hypothesis of constant input power equal to 20 mW. A maximum output power of 30 W was obtained for an input signal of 20 mW at 17 GHz. In this specific condition, the gain is equal to 31.8 dB, reaching an electronic efficiency of 15.5 %. The gain for the unit cell and unit length, in the optimal condition, is equal to 0.318 dB and 0.795 dB/mm, respectively. The power of the output signal overcomes 20 W in the range of frequency from 15.5 to 17.8 GHz, and overcomes 10 W in the range

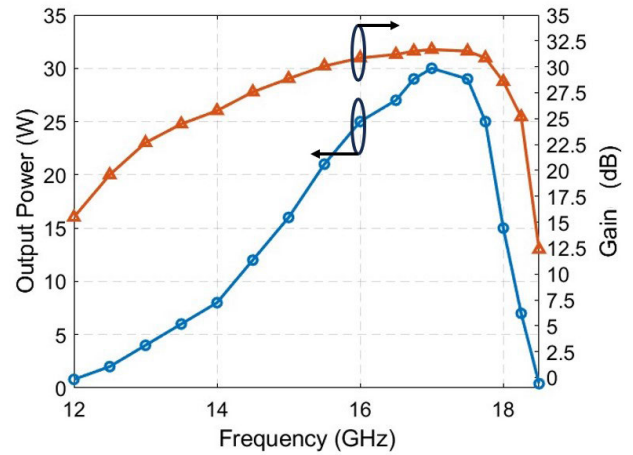


FIGURE 13. Gain (blue) and Output Power (orange) Vs frequency.

from 14.2 to 18.2 GHz. The -3 dB bandwidth is 3.2 GHz, from 14.8 to 18 GHz.

V. CONCLUSION

In this article, the design of a low-voltage and high power TWT, based on a modified rectangular RBSWS, is proposed. The proposed structure has been first compared with a low voltage version of the classic circular RBSWS, showing a larger interaction impedance and, hence, allowing to reach higher power output. Moreover, the proposed structure shows a flatter phase velocity, ensuring a greater stability. By optimizing the dimensions of the couplers, a reflection coefficient lower than -10 dB and a transmission coefficient higher than -1 dB were obtained in the frequency range of interest. The beam-wave interaction is evaluated with the use of the 3D Solver PIC of CST Studio suite 2023. The output power of the optimized structure overcomes 30 W, with a unit gain of 0.795 dB/mm which means a total gain higher than 30 dB. Moreover, the proposed structure shows a great stability with a high rejection of backward wave oscillations. Finally, unlike other structures, our configuration presents a very large surface between the dielectric and the SWS, which allows a great mechanical and thermal stability. Future activities will focus on the fabrication of the RRB-SWS described in this paper.

REFERENCES

- [1] C. Paoloni, D. Gamzina, R. Letizia, Y. Zheng, and N. C. Luhmann, "Millimeter wave traveling wave tubes for the 21st century," *J. Electromagn. Waves Appl.*, vol. 35, no. 5, pp. 567–603, Mar. 2021, doi: [10.1080/09205071.2020.1848643](https://doi.org/10.1080/09205071.2020.1848643).
- [2] G. Watson, *Principles of Electron Tubes*. Princeton, NJ, USA: Van Nostrand Reinhold Inc., 1965.
- [3] D. J. Radack, J. H. Booske, Y. Carmel, and W. W. Destler, "Wiggler focused relativistic sheet beam propagation in a planar free-electron laser configuration," *Appl. Phys. Lett.*, vol. 55, no. 20, pp. 2069–2071, Nov. 1989, doi: [10.1063/1.102108](https://doi.org/10.1063/1.102108).
- [4] G. V. Torgashov, R. A. Torgashov, V. N. Titov, A. G. Rozhnev, and N. M. Ryskin, "Meander-line slow-wave structure for high-power millimeter-band traveling-wave tubes with multiple sheet electron beam," *IEEE Electron Device Lett.*, vol. 40, no. 12, pp. 1980–1983, Dec. 2019, doi: [10.1109/LED.2019.2945502](https://doi.org/10.1109/LED.2019.2945502).

- [5] C. D. Joye, A. N. Vlasov, R. Jaynes, I. A. Chernyavskiy, K. T. Nguyen, J. Pasour, J. C. Rodgers, F. N. Wood, V. Jabotinski, T. M. Antonsen, S. J. Cooke, A. M. Cook, and B. Levush, "Ka-band low-voltage multiple-beam mini-TWT," *IEEE Trans. Electron Devices*, vol. 70, no. 6, pp. 2828–2833, Jun. 2023, doi: [10.1109/TED.2023.3239839](https://doi.org/10.1109/TED.2023.3239839).
- [6] R. Yang, L. Yue, J. Xu, P. Yin, J. Luo, H. Wang, D. Jia, J. Zhang, H. Yin, J. Cai, G. Guo, G. Zhao, W. Wang, D. Li, and Y. Wei, "Broadband-printed traveling-wave tube based on a staggered rings microstrip line slow-wave structure," *Electronics*, vol. 11, no. 3, p. 384, Jan. 2022, doi: [10.3390/electronics11030384](https://doi.org/10.3390/electronics11030384).
- [7] C. Chua, J. M. Tsai, S. Aditya, M. Tang, S. W. Ho, Z. Shen, and L. Wang, "Microfabrication and characterization of W-band planar helix slow-wave structure with straight-edge connections," *IEEE Trans. Electron Devices*, vol. 58, no. 11, pp. 4098–4105, Nov. 2011, doi: [10.1109/TED.2011.2165284](https://doi.org/10.1109/TED.2011.2165284).
- [8] C. Zhao, S. Aditya, and C. Chua, "Symmetric planar helix slow-wave structure with straight-edge connections for application in TWTs," in *Proc. IEEE Int. Vac. Electron. Conf.*, Apr. 2014, pp. 291–292, doi: [10.1109/IVEC.2014.6857604](https://doi.org/10.1109/IVEC.2014.6857604).
- [9] S. Wang and S. Aditya, "Design of a Ka-band microfabricated PH-SEC slow-wave structure with coplanar waveguide couplers," in *Proc. IEEE Region 10 Conf. (TENCON)*, Nov. 2016, pp. 3684–3687, doi: [10.1109/TENCON.2016.7848745](https://doi.org/10.1109/TENCON.2016.7848745).
- [10] Z. Wen, J. Luo, Y. Li, W. Guo, and M. Zhu, "A concentric arc meander line slow wave structure applied on low voltage and high efficiency Ka-band TWT," *IEEE Trans. Electron Devices*, vol. 68, no. 3, pp. 1262–1266, Mar. 2021, doi: [10.1109/TED.2020.3047592](https://doi.org/10.1109/TED.2020.3047592).
- [11] S. Wang, Y. Gong, Z. Wang, Y. Wei, Z. Duan, and J. Feng, "Study of the symmetrical microstrip angular log-periodic meander-line traveling-wave tube," *IEEE Trans. Plasma Sci.*, vol. 44, no. 9, pp. 1787–1793, Sep. 2016, doi: [10.1109/TPS.2016.2598614](https://doi.org/10.1109/TPS.2016.2598614).
- [12] S. Wang, Y. Gong, Y. Hou, Z. Wang, Y. Wei, Z. Duan, and J. Cai, "Study of a log-periodic slow wave structure for Ka-band radial sheet beam traveling wave tube," *IEEE Trans. Plasma Sci.*, vol. 41, no. 8, pp. 2277–2282, Aug. 2013, doi: [10.1109/TPS.2013.2271639](https://doi.org/10.1109/TPS.2013.2271639).
- [13] X. Li, Y. Xu, S. Wang, Z. Wang, X. Shi, Z. Duan, Y. Wei, J. Feng, and Y. Gong, "Study on phase velocity tapered microstrip angular log-periodic meander line travelling wave tube," *IET Microw., Antennas Propag.*, vol. 10, no. 8, pp. 902–907, Jun. 2016, doi: [10.1049/iet-map.2015.0520](https://doi.org/10.1049/iet-map.2015.0520).
- [14] S. Stivala, G. Lipari, G. Paterna, E. Traina, R. Dionisio, A. Busacca, A. Muratore, and P. Livreri, "Design of a planar helix slow wave structure for TWT applications in the K-band," in *Proc. 24th Int. Vac. Electron. Conf. (IVEC)*, Chengdu, China, Apr. 2023, pp. 1–2, doi: [10.1109/IVEC56627.2023.10157333](https://doi.org/10.1109/IVEC56627.2023.10157333).
- [15] A. S. Gilmour Jr., *Microwave and Millimeter-Wave Vacuum Electron Devices*. Boston, MA, USA: Artech House, 2020.
- [16] J. F. Gittins, *Power Travelling-Wave Tubes*. New York, NY, USA: American Elsevier Publishing Company, 1965.
- [17] C. Chua, S. Aditya, J. M. Tsai, M. Tang, and Z. Shen, "Microfabricated planar helical slow-wave structures based on straight-edge connections for THz vacuum electron devices," *THz Sci. Technol.*, vol. 4, pp. 208–229, Dec. 2011.
- [18] C. Chua, S. Aditya, and Y. Y. Lau, "W-band rectangular ring-bar structure with straight-edge connections," in *Proc. IEEE 14th Int. Vac. Electron. Conf. (IVEC)*, Paris, France, May 2013, pp. 1–2, doi: [10.1109/IVEC.2013.6570893](https://doi.org/10.1109/IVEC.2013.6570893).
- [19] W. Wei, C. Yu, Y. Wei, M. Tan, Z. Lu, M. Lu, and W. Wang, "Novel rectangular-ring vertex double-bar slow wave structure for high-power high-efficiency traveling-wave tubes," *IEEE Trans. Electron Devices*, vol. 68, no. 12, pp. 6512–6517, Dec. 2021, doi: [10.1109/TED.2021.3120693](https://doi.org/10.1109/TED.2021.3120693).
- [20] W. Wei, S. Wang, Y. Wei, W. Hu, L. Zhang, Y. Dong, Z. Lu, Y. Jiang, and W. Wang, "Square- and rectangular-ring vertex-bar slow wave structures for high-efficiency wide bandwidth TWTs," *IEEE Trans. Electron Devices*, vol. 70, no. 1, pp. 296–301, Jan. 2023, doi: [10.1109/TED.2022.3225138](https://doi.org/10.1109/TED.2022.3225138).
- [21] J. M. Honig, *Thermodynamics Principles Characterizing Physical and Chemical Processes*, 5th ed. New York, NY, USA: American Elsevier Publishing Company, Sep. 2020.
- [22] D. Zhao, X. Lu, Y. Liang, X. Yang, C. Ruan, and Y. Ding, "Researches on an X-band sheet beam klystron," *IEEE Trans. Electron Devices*, vol. 61, no. 1, pp. 151–158, Jan. 2014, doi: [10.1109/TED.2013.2291781](https://doi.org/10.1109/TED.2013.2291781).



G. PATERNA received the B.S. and M.S. degrees in electronics engineering from the University of Palermo (UNIPA), Italy, in 2020 and 2023, respectively, where he is currently pursuing the Ph.D. degree in information and communication technologies. Since 2022, he has been focusing mostly on the study and design of vacuum electron tubes, mostly high power microwave devices. His research interests include microwave slow-wave structures, electron guns, and microwave devices.



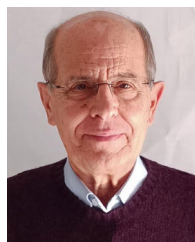
G. LIPARI received the B.S. and M.S. degrees in electronics engineering from the University of Palermo (UNIPA), Italy, in 2020 and 2023, respectively, where he is currently pursuing the Ph.D. degree in information and communication technologies. Since 2022, he has been focusing mostly on the study and design of vacuum electron tubes, mostly TWTs for space applications. His research interests include microwave slow-wave structures, electron guns, and microwave devices.



E. TRAINA received the B.S. and M.S. degrees in electronics engineering from the University of Palermo, Italy, in 2020 and 2023, respectively, where she is currently pursuing the Ph.D. degree in space science and technology. Since 2022, she has been focusing mostly on the study and design of vacuum electron tubes, mostly extended interaction klystrons. Her research interests include microwave slow-wave structures, electron guns, and microwave devices.



G. COMPARATO received the bachelor's degree in cybernetics engineering, in 2022. She is currently pursuing the master's degree in electronic engineering with the University of Palermo (UNIPA), Italy, and working on a thesis in the microwave field. Since then, she continued to study focusing on vacuum electronics.



A. MURATORE received the master's degree in electronic engineering, in 1973. He has been a Senior Designer and a Lecturer of microwave electronics with the Department of Engineering, University of Palermo (UNIPA), Italy, since 2020. He has a background of more than 30 years, working in vacuum electronics with Leonardo S.p.A., covering also the position of the Manager. During this period, he has developed and designed many vacuum microwave devices.



P. LIVRERI (Senior Member, IEEE) received the Laurea degree (Hons.) in electronics engineering and the Ph.D. degree in electronics and communications engineering from the University of Palermo, Italy, in 1986 and 1992, respectively. From 1993 to 1994, she was a Researcher with the National Council for Researches, CNR, Rome, Italy. Since 1995, she has been the Scientific Director for the Microwave Instruments and Measurements Laboratory, Department of Engineering, University of Palermo. In 2020, she joined the CNIT National Laboratory for Radar and Surveillance Systems RaSS, Pisa. She is currently a Professor with the Department of Engineering, University of Palermo; and a Visiting Professor with the San Diego State University. She is a Principal Investigator of the “Microwave Quantum Radar” project, funded by the Ministry of Defense, in 2021. She is the author or coauthor of more than 200 publications on prestigious international journals and conferences. Her research interests include microwave and millimeter vacuum high power (TWT and Klystron) and solid-state power amplifiers for radar applications, high power microwave sources (virtual cathode oscillator and magnetically insulated transmission line oscillator), microwave and optical antennas, radar, and microwave quantum radar.



S. STIVALA received the master’s degree in electronic engineering and the Ph.D. degree in electronic and telecommunication engineering from the University of Palermo, (UNIPA), Italy, in 2004 and 2008, respectively. He has been an Associate Professor of electronics with the Department of Engineering, UNIPA, since July 2020. He is the Coordinator of the master’s degree program in electronics engineering (since December 2022) and a member of the Ph.D. board in “Information and Communication Technologies.” He has been an advisor of three Ph.D. candidates and a supervisor of more than 30 bachelor’s and master’s Thesis. He is the author or coauthor of about 100 publications on prestigious international journals and conferences. His main research interests include design and characterization of RF/microwave devices and circuits, terahertz spectroscopy, optical and electrical characterization of photodetectors, optoelectronic devices, biophotonics, and error mitigation in free-space optical communications.



A. BUSACCA received the master’s degree in electronic engineering and the Ph.D. degree in electronic, computer and telecommunication engineering from the University of Palermo (UNIPA), Italy, in 1998 and 2002, respectively. He has been a Full Professor of electronics with the Department of Engineering, UNIPA, since September 2018. He has involved as a WP leader or a Coordinator in several projects, financed from private industries, the Italian Ministry of University and Research, the Italian and the European Space Agency, and the European Community. He is the author or coauthor of more than 180 publications on prestigious international journals and conferences. His main research interests include power electronics, power converters, characterization of SiC and GaN devices for automotive applications, LIDAR and sensors for autonomous drive, photodetectors characterization, photonic microtechnologies, optical fiber devices, linear and nonlinear integrated optical devices, optoelectronic devices, design and realization of multisensor wearable devices for biomedical applications, free space optics communication, fabrication and characterization of photovoltaic cells, and terahertz science.

...